

**Corresponding author:**

Dr. Hong-Jian Feng

Department of Applied Physics,

School of Science,

Chang'an University,

Xi'an 710064, China

Tel.: +86-29-82337620

Email address:

fenghongjian@gmail.com

fenghongjian1978@gmail.com

# The reversal of magnetization driven by the Dzyaloshinskii-Moriya interaction(DMI) in perovskite $\text{Bi}_2\text{FeMnO}_6$

Hong-Jian Feng

*Department of Applied Physics, School of Science, Chang'an University, Xi'an  
710064, China*

---

## Abstract

*Ab initio* calculations show that the coupling between antiferrodistortive(AFD) distortions and magnetization in perovskite  $\text{Bi}_2\text{FeMnO}_6$  is prohibited to make magnetization rotate as on-site Coulomb interaction( $U$ ) is larger than 2.7 eV, where anomalies in antiferromagnetic(AFM) vectors and band gap varying with on-site Coulomb interaction can be observed. This coupling is attributed to the antisymmetric Dzyaloshinskii-Moriya interaction(DMI) driven by the  $e_g$ - $e_g$  states AFM interaction and charge redistribution with respect to different AFD distortions.

*Key words:* Dzyaloshinskii-Moriya interaction(DMI);On-site Coulomb Interaction ; $\text{Bi}_2\text{FeMnO}_6$

*PACS:* 75.30.Et,75.30.GW,71.15.Mb

---

## 1 Introduction

Multiferroics are materials in which ferroic properties, e.g., magnetism and polar order coexist. Magnetic and ferroelectric ordering couple microscop-

ically or macroscopically to form the magnetic ferroelectrics. The coupling of the two ordering leads to the so-called magnetoelectric effect in which the magnetization can be tuned by the external electric field, and vice versa[1,2,3]. Magnetic ferroelectrics have potential applications in information storage, actuators, sensors, and functional devices. Perovskite  $\text{BiFeO}_3$  exhibits both weak ferromagnetism and ferroelectric characteristics, and has been studied extensively in recent days.[4,5,6,7,8]. The G-type antiferromagnetic (AFM) order of Fe magnetic moments exhibits a canting caused by the antisymmetric Dzyaloshinskii-Moriya interaction(DMI) under rhombohedral  $R3c$  space group. However, a spiral spin structure of AFM Fe sublattice rotates through the crystal with a long-wavelength period of  $620\text{\AA}$ , and decrease the weak ferromagnetism further. In our previous work, we suggested that the effect of decreasing magnetism caused by the spiral spin structure can be suppressed by doping magnetic transitional metal ions in perovskite B sites[9]. We suggest perovskite  $\text{Bi}_2\text{FeMnO}_6$  is a good candidate to fulfill this requirement in that Mn and Fe have different magnetic moments and hence lower DMI to produce the rotation of AFM vectors. Comparing with  $\text{BiFeO}_3$ , the new system should have an observed magnetization and reversal of magnetization macroscopically. Except the ferroelectric displacement of Bi site driven by Bi-6s stereochemically active lone pair induced by the mixing between the  $(ns)^2$  ground state and a low-lying  $(ns)^1(np)^1$  excited state, there exists another structural distortion, the alternating sense of rotation of the oxygen octahedra along  $[1\ 1\ 1]$  direction, which is known as antiferrodistortive(AFD) distortion [10,11]. Also in our former paper, it is shown that AFD distortion couples with the weak ferromagnetism due to the DMI which is decreasing with increasing on-site Coulomb interaction( $U$ ) [12]. We aim to extend our study to perovskite  $\text{Bi}_2\text{FeMnO}_6$  to investigate the coupling between AFD distortion and weak ferromagnetism under DMI using *ab initio* calculations with considering the

spin-orbital(SO) coupling effect and the noncollinear spin configuration, while Mn were doped periodically along [1 1 1] direction in Fe site of  $\text{BiFeO}_3$ . Does AFD distortion couple with magnetism in  $\text{Bi}_2\text{FeMnO}_6$  when Fe and Mn are arranged in G-type AFM ordering? What is the origin of coupling between the AFD distortion and the magnetism under DMI in  $\text{Bi}_2\text{FeMnO}_6$ ? What is the role of DMI in the coupling between AFD distortion and magnetization? How does Coulomb interaction( $U$ ) take effect on the DMI? In this paper we have proposed the mechanism of DMI in  $\text{Bi}_2\text{FeMnO}_6$ , using first-principles calculations based on density functional theory(DFT). This work can shed light on discovering the magnetoelectric coupling process in perovskite multiferroics.

The remainder of this paper is organized as follows: In section 2, we presented the computational details of our calculations. We reported the calculated results and discussions in section 3. In section 4, we drew conclusion based on our calculation.

## 2 Computational details

Our calculations were performed within the local spin density approximation(LSDA) to DFT using the ABINIT package[13,14]. The ion-electron interaction was modeled by the projector augmented wave (PAW) potentials [15,16] with a uniform energy cutoff of 500 eV. Bi 5d, 6s, and 6p electrons, Fe 4s, 4p, and 3d electrons, and O 2s and 2p electrons were considered as valence states. Two partial waves per  $l$  quantum number were used. The cutoff radii for the partial waves for Bi, Fe, and O were 2.5, 2.3, 1.1 a.u., respectively.  $6 \times 6 \times 6$  Monkhorst-Pack sampling of the Brillouin zone were used for all calculations. We calculated the net magnetization per unit cell and the electronic properties within the LSDA+U method where the strong Coulomb repulsion

between localized  $d$  states has been considered by adding a Hubbard-like term to the effective potential[17,18,19]. The effective Hubbard parameter, the difference between the Hubbard parameter  $U$  and the exchange interaction  $J$  ( $U - J$ ), was changing in the range between 0 and 5 eV for the Fe and Mn  $d$  states. For 0 eV of ( $U - J$ ),  $J$  was varying as 0,0.5, 0.8, and 1 eV, respectively.  $J$  remained 1 eV for other effective Hubbard values. Taking into account the SO interaction, we introduced the noncollinear spin configuration to construct the G-type AFM magnetic order with the AFM axis being along the  $x$  axis in Cartesian coordinates in our *ab initio* calculation.

### 3 Results and discussion

The initial lattice parameters are introduced as same as BiFeO<sub>3</sub> in Ref.[4]. Then cell shape and the atomic positions are fully relaxed, and the relaxed parameters are given in table 1. One can see that the lattice constant is decreased with doping Mn in BiFeO<sub>3</sub>. The rhombohedral angle is also decreased comparing with BiFeO<sub>3</sub>. This shows that the lattice cell is compressed with substitution of Mn in Fe site while lattice shape is also changed with decreasing rhombohedral angle.

For the AFD distortion, a rotational vector  $\mathbf{R}$  has been introduced to describe the direction of the rotation of the oxygen octahedra[12].  $\mathbf{R}_{out}$  corresponds to the state in which the rotational vectors of two neighboring oxygen octahedra are deviating away, while  $\mathbf{R}_{in}$  is pointing inward. The rotational angle is 10° in the Cartesian coordinates[12].  $U$  and  $J$  are the Coulomb interaction and superexchange interaction parameter which were implemented in LSDA+U calculation as in ref.[12].  $U$  is the amount of energy required to transfer one electron from one site to its nearest neighbor, while  $J$  indicates

the strength of the magnetic superexchange interaction.

In table 2, we present the net magnetization per unit cell with respect to  $\mathbf{R}_{in}$  and  $\mathbf{R}_{out}$  in Cartesian coordinates for different  $U$  and  $J$ . For the sake of clarity, we only set varying value of  $J$  for  $U=0$  eV. Again, one can see that  $J$  value have no effect on the resulting magnetization when  $U$  remains constant. The initial magnetic moment of Fe are arranged in ferrimagnetic order along  $x$  direction which is known as G-type AFM order. The resultant magnetic moment in  $x$  direction is due to the ferrimagnetic arrangement of Fe and Mn magnetization. The neighboring moment will interact under the DMI and deviate away from the original  $x$  direction to produce a resultant magnetic moment in  $y$  direction. When the rotational vector  $\mathbf{R}$  is reversed, the resultant magnetic moment will be reversed too until the  $U$  is smaller than 2.7 eV. This indicates the AFD and magnetic ordering is coupled and DMI is still active in this case. As  $U$  is greater than 2.7 eV, the coupling between these two ordering is prohibited. That is to say, the DMI is precluded in this case. It is worth mentioning that the component of magnetic moment in  $y$  direction for  $U = 2.7$  eV becomes zero. This indicates the critical value of  $U$  for depressing DMI is 2.7 eV in which the antisymmetric Fe and Mn magnetic moments stop interacting with each other. This critical value is smaller than that for  $\text{BiFeO}_3$  where the DMI is turned off as  $U$  is approaching 2.9 eV[12]. This indicates that Fe-Mn antisymmetric interaction where interacting spin moment are  $(5/2)S - (4/2)S$  is weaker than Fe-Fe antisymmetric interaction where interacting spin moment are  $(5/2)S - (5/2)S$ . We believe the weaker DMI and alternating spin moments in the new system would destroy the spiral spin structure through the crystal in comparison with the case in  $\text{BiFeO}_3$ . Hereby the magnetization and reversal of magnetization can be improved in the new system. In order to make the reversal of magnetization clear, the resultant AFM vectors are illustrated in Fig.1 with respect to  $U$ . AFM vectors

have three components corresponding to  $x$ ,  $y$ , and  $z$  direction, respectively. It is apparent that there is an anomaly as  $U$  is approaching 2.7 eV which corresponds to the critical value of eliminating DMI. The magnetization is inverted as  $U$  is under the critical value which indicates the DMI is still active in this  $U$  range. Meanwhile the DMI is inversely proportional to the  $U$  value. The deviation of original magnetic moment away from  $x$  axis only occurs in  $xoy$  plane. That is why the reversal of magnetic moment can not be observed in  $z$  direction.

The relationship between DMI and Coulomb on-site interaction can be understood theoretically as follows. The Hamiltonian of the new perovskite system reads,

$$H_{Bi_2FeMnO_6} = -2 \sum_{\langle Fei, Mnj \rangle} \mathbf{J}_{Fei, Mnj} \mathbf{S}_{Fei} \cdot \mathbf{S}_{Mnj} + \sum_{\langle Fei, Mnj \rangle} \mathbf{D}_{Fei, Mnj} \mathbf{S}_{Fei} \times \mathbf{S}_{Mnj}. \quad (1)$$

The first term is attributed to the symmetric superexchange, and the second term is the antisymmetric DMI contribution which only occurs when the inversion symmetry of the cations is broken. The constant  $\mathbf{D}$  is related to the AFD displacement and the rotational vector. It functions like a 'DMI constant' which indicates the strength of the DMI. It reads by the second order perturbation in the case of one electron per ion

$$\mathbf{D}_{Fe, Mn}^{(2)} = (4i/U)[b_{nn'}(Fe-Mn)C_{n'n}(Mn-Fe) - C_{nn'}(Fe-Mn)b_{n'n}(Mn-Fe)], \quad (2)$$

From this relation, it can be seen that the DMI constant is inversely proportional to the on-site Coulomb interaction and has nothing to do with the symmetric superexchange parameter.

The new system should possess a good insulating property in terms of the band gap calculated, and hence a reversal states of ferroelectricity. The band

gap for metal oxides can be opened with adopting an appropriate  $U$  value. The corresponding value for  $\text{BiFeO}_3$  is about 4.3 eV. We take 5 eV  $U$  value for Fe and Mn in  $\text{Bi}_2\text{FeMnO}_6$  to analyze the total density of states(DOS) in that the band gap can be increased slightly with increasing  $U$  value. The band gap corresponding to two rotational vectors are demonstrated in Fig.2. Generally, the band gap corresponding to the two rotational vectors are increasing linearly with respect to  $U$  value, while there exist two anomalies to the two AFD states as  $U$  approaching 2.7 eV where the band gap are disappeared. These anomalies in the curve are consistent with the calculating results for AFM vectors shown in table 2 and Fig. 1, respectively. The anomalies show the disappearance of DMI occurs at the critical  $U$  value and is caused by the hopping of electrons through Fermi energy. Moreover, the band gap to  $\mathbf{R}_{out}$  is more narrower than to  $\mathbf{R}_{in}$  which is probably caused by the different ligand field related with structure. In comparison with the total DOS without applying the on-site Coulomb interaction, the total DOS with  $U$  value of 5 eV is shown in Fig. 3. The finite DOS in the vicinity of Fermi level is pushed away to form the band gap as  $U$  is equal to 5 eV. A 1.26 eV and 0.75 eV band gap is obtained for  $\mathbf{R}_{out}$  and  $\mathbf{R}_{in}$  rotational states, respectively. This indicates that these two AFD states both possess a semiconducting property. A ferroelectric reversal would be expected to these two reversal AFD states. However,  $\text{Bi}_2\text{FeMnO}_6$  remains metal property without applying  $U$ . Again this shows that the on-site Coulomb interaction is significant in opening the band gap for perovskite metal oxides.

In order to shed light on the role of DMI between neighboring Fe and Mn ions, we report the orbital resolved density of states(ODOS) of the magnetic ions as  $U$  is equal to 2.6 eV which is exactly under the critical value for precluding the antisymmetric DMI. The ODOS of Fe and Mn corresponding to  $\mathbf{R}_{out}$  and  $\mathbf{R}_{in}$  states are shown in Fig. 4. It is apparent that there are large



amount of doubly degenerate  $e_g$  states for Fe and Mn in the occupied bands around the vicinity of the Fermi level. The charge hybridization between Fe-3d and Mn-3d electrons is realized mainly by the  $e_g$ - $e_g$  states interaction. It suggests that the  $e_g$ - $e_g$  AFM interaction play an important role in the anti-symmetric DMI between Fe and Mn ions.  $e_g$  state is composed by  $d_{z^2-r^2}$  and  $d_{x^2-y^2}$  orbitals. It is worth mentioning that the finite ODOS in the vicinity of Fermi level is mainly attributed to the  $d_{z^2-r^2}$  orbital. We suggest that  $e_g$ - $e_g$  AFM interaction is exactly mediated by neighboring  $d_{z^2-r^2}$  orbitals of Fe and Mn ions. The charge transformation between Fe and Mn ions, and hence the inversion of magnetization can be seen from Fig. 5. The hopping of electrons between neighboring  $e_g$ - $e_g$  pairs occurs due to the DMI as the inversion symmetry of cations is broken. Moreover the hopping of electrons couples with the rotation of the neighboring oxygen octahedra to produce the resultant magnetization. The charge distribution in neighboring  $e_g$ - $e_g$  states is polarized to a certain rotational vector, and the charge distribution is inversely polarized as the rotational vector is changing direction, leading to the reversal of resultant magnetization eventually. The charge distribution is supposed to distribute uniformly without applying the DMI. However, the homogenous distribution is destroyed by the DMI between neighboring magnetic ions to form a polarized status. We suggest this constitutes the microscopic mechanism of DMI in perovskite multiferroics. On the other hand, the AFM interaction in triply degenerate  $t_{2g}$ - $t_{2g}$  composed by  $d_{xy}$ ,  $d_{yz}$ , and  $d_{xz}$  orbitals is relatively weak comparing with  $e_g$ - $e_g$  AFM interaction. Again this shows that the latter is deeply involved in the antisymmetric DMI.

## 4 Conclusion

The critical value of  $U$  for depressing DMI in  $\text{Bi}_2\text{FeMnO}_6$  is found to be 2.7 eV which is smaller than that in  $\text{BiFeO}_3$ . This indicates that the DMI in the new system functions weaker in comparison with that in  $\text{BiFeO}_3$ . ODOS of Fe and Mn corresponding to different AFD displacements show that the microscopic mechanism of the DMI is originating from the hopping of electrons between neighboring  $e_g$ - $e_g$  states, and the  $e_g$ - $e_g$  AFM interaction couples with the rotation of the neighboring oxygen octahedra.

## References

- [1] G. Maugin, Phys.Rev.B 23(1981)4608.
- [2] H. Schmid, Ferroelectrics 162 (1994)317.
- [3] M. Fiebig, J.Phys.D:Appl. Phys. 38(2005)R123.
- [4] J. Wang, J. B. Neaton, H. Zheng, V. Nagarajan, S. B. Ogale, B. Liu, D. Viehland, V. Vaithyanathan, D. G. Schlom, U. V. Waghmare, N. A. Spaldin, K. M. Rabe, M. Wuttig, R. Ramesh, Science 299(2003)1719.
- [5] Hong-Jian Feng, J. Mag. Mag. Mater. 322(2010)3755.
- [6] R. Ranjith, U. Lüders, W. Prellier, A. Da Costa, I. Dupont, R. Desfeus, J. Mag. Mag. Mater. 321(2009)1710.
- [7] P. Rovillain, M. Cazayous, A. Sacuto, D. Lebeugle, D. Colson, J. Mag. Mag. Mater. 321(2009)1699.
- [8] Manoj K. Singh, S. Dussan, W. Prellier, Ram s., Katiyar, J. Mag. Mag. Mater. 321(2009)1706.
- [9] Hong-Jian Feng, F. Liu, Phys. Lett. A 372(2008) 1904.

- [10] C. Ederer, N. A. Spaldin, Phys. Rev. B 71(2005)060401.
- [11] Hong-Jian Feng, F. Liu, Chin.Phys. Lett. 25(2008) 671.
- [12] Hong-Jian Feng, J. Mag. Mater. 322(2010)1765.
- [13] The ABINIT code is a common project of the Universite Catholique de Louvain, Corning, Inc., and other contributors(URL <http://www.abinit.org>).
- [14] X. Gonze, J.-M. Beuken , R. Caracas, F. Detraux, M. Fuchs, G.-M. Rignanes, F. Jollet, M. Torrent, A. Roy, M. Mikami, P. Ghosez, J.-Y. Raty , D. C. Alan,Comp. Mater. Sci. 25(2002)478.
- [15] P. E. Blochl,Phys. Rev. B 50(1994)17953.
- [16] G. Kresse, D. Joubert,Phys. Rev. B 59(1999)1758.
- [17] V. I. Anisimov, J. Zaane, O. K. Andersen,Phys. Rev. B 44(1991)943.
- [18] V. I. Anisimov, I. V. Solovyev, M. A. Korotin, Phys. Rev. B 48(1993) 16929.
- [19] V. I. Anisimov, F. Aryasetiawan, A. I. Lichtenstein,J. Phys.: Condens. Matter. 9(1997)767.

Table 1

Calculated lattice constant  $a$ , rhombohedral angle  $\alpha$ , volume  $V$ , and Wyckoff parameters for  $\text{Bi}_2\text{FeMnO}_6$ . The Wyckoff positions  $1a(x,x,x)$  for the cations and  $3b(x,y,z)$  for the anions.

		$\text{Bi}_2\text{FeMnO}_6$	$\text{BiFeO}_3$
$a(\text{\AA})$		5.030	5.459
$\alpha(^{\circ})$		59.02	60.36
$V(\text{\AA}^3)$		105.57	115.98
Bi	x	-0.012/0.489	0.000
Fe/Ti	x	0.226(Fe)/0.727(Mn)	0.231
O	x	0.541	0.542
	y	0.950	0.943
	z	0.406	0.398

Table 2

Magnetization per unit cell with respect to different value of  $U$  and  $J$ .

$U(eV)$	0		0.5		0.8		1		2	
$J(eV)$	0		0.5		0.8		1		1	
	$\mathbf{R}_{in}$	$\mathbf{R}_{out}$	$\mathbf{R}_{in}$	$\mathbf{R}_{out}$	$\mathbf{R}_{in}$	$\mathbf{R}_{out}$	$\mathbf{R}_{in}$	$\mathbf{R}_{out}$	$\mathbf{R}_{in}$	$\mathbf{R}_{out}$
$M_x(\mu_B)$	-2.9723	1.0683	-2.9723	1.0683	-2.9723	1.0683	-2.9723	1.0683	-2.9775	1.0041
$M_y(\mu_B)$	-0.0079	0.0887	-0.0079	0.0887	-0.0079	0.0887	-0.0079	0.0887	-0.0100	0.0367
$M_z(\mu_B)$	0.0004	0.0071	0.0004	0.0071	0.0004	0.0071	0.0004	0.0071	0.0021	0.0025
$U(eV)$	3		3.5		3.6		3.7		3.8	
$J(eV)$	1		1		1		1		1	
	$\mathbf{R}_{in}$	$\mathbf{R}_{out}$	$\mathbf{R}_{in}$	$\mathbf{R}_{out}$	$\mathbf{R}_{in}$	$\mathbf{R}_{out}$	$\mathbf{R}_{in}$	$\mathbf{R}_{out}$	$\mathbf{R}_{in}$	$\mathbf{R}_{out}$
$M_x(\mu_B)$	-2.9813	1.0159	-2.9843	1.0126	-2.9846	1.0108	-2.9851	1.0087	-2.9856	1.0118
$M_y(\mu_B)$	-0.0050	0.0208	-0.0013	0.0194	-0.0004	0.0205	0.0000	0.0211	0.0002	0.0238
$M_z(\mu_B)$	0.0021	-0.0008	0.0013	-0.0004	0.0011	0.0001	0.0009	0.0009	0.0003	0.0017
$U(eV)$	3.9		4		5		6			
$J(eV)$	1		1		1		1			
	$\mathbf{R}_{in}$	$\mathbf{R}_{out}$	$\mathbf{R}_{in}$	$\mathbf{R}_{out}$	$\mathbf{R}_{in}$	$\mathbf{R}_{out}$	$\mathbf{R}_{in}$	$\mathbf{R}_{out}$	$\mathbf{R}_{in}$	$\mathbf{R}_{out}$
$M_x(\mu_B)$	-2.9862	1.0115	-2.9866	1.0115	-2.9919	1.0093	-2.9921	1.0074		
$M_y(\mu_B)$	0.0007	0.0231	0.0011	0.0233	0.0090	0.0220	0.123	0.0144		
$M_z(\mu_B)$	0.0003	0.0025	0.0000	0.0025	0.0000	0.0018	-0.0003	0.0013		

**Figure captions:**

Fig.1 Relationship between AFM vectors and  $U$  .

Fig.2 Band gap as a function of  $U$  .

Fig.3 Total DOS for  $\mathbf{R}_{in}$  and  $\mathbf{R}_{out}$  with  $U=5$  eV and without applying  $U$  .

Fig. 4 ODOS of Fe and Mn for  $\mathbf{R}_{in}$  and  $\mathbf{R}_{out}$  with  $U=2.6$  eV and without applying  $U$  .

Fig. 5 Schematic diagram for rotation of magnetization and DMI between the neighboring Fe and Mn ions in  $\text{Bi}_2\text{FeMnO}_6$ . The arrow denote the magnetic moment.

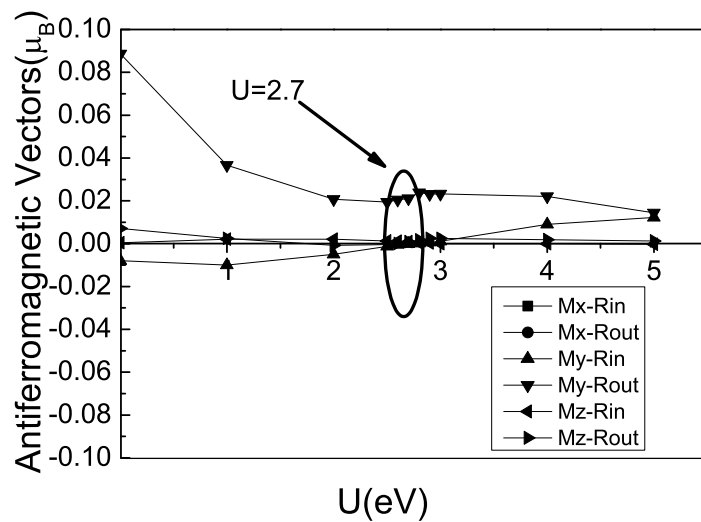


Fig. 1. Relationship between AFM vectors and  $U$  .

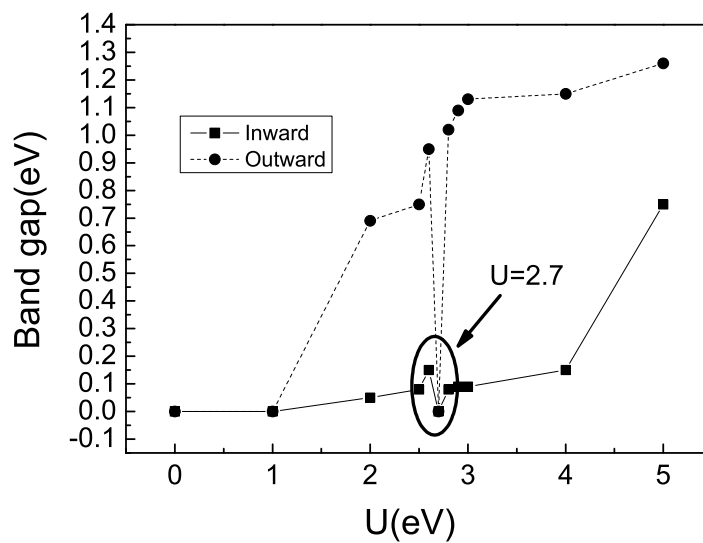


Fig. 2. Band gap as a function of  $U$ .

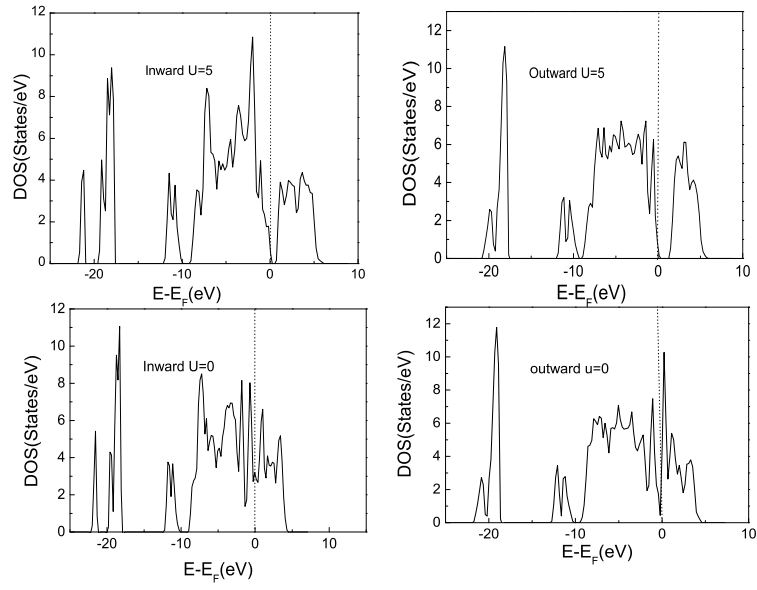


Fig. 3. Total DOS for  $\mathbf{R}_{in}$  and  $\mathbf{R}_{out}$  with  $U=5$  eV and without applying  $U$ .



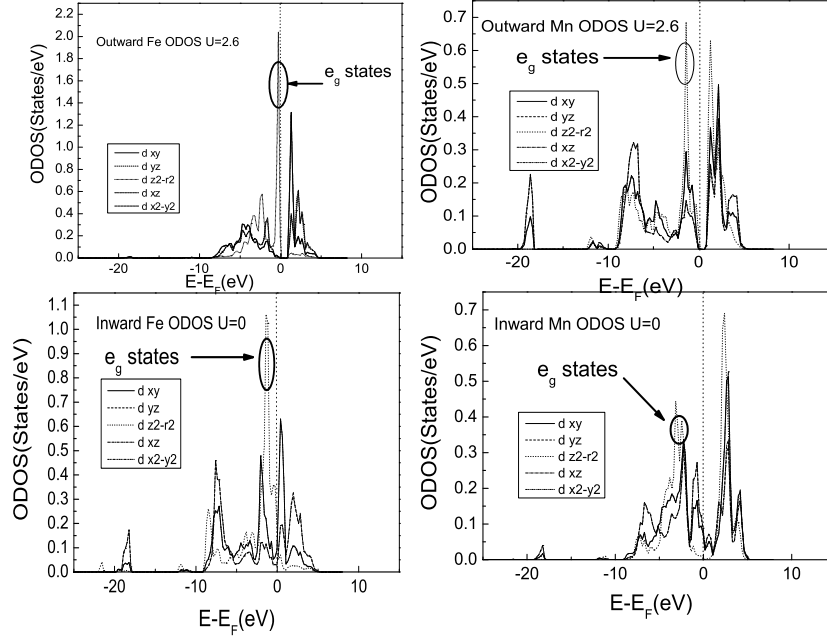


Fig. 4. ODOS of Fe and Mn for  $\mathbf{R}_{in}$  and  $\mathbf{R}_{out}$  with  $U=2.6$  eV and without applying  $U$ .

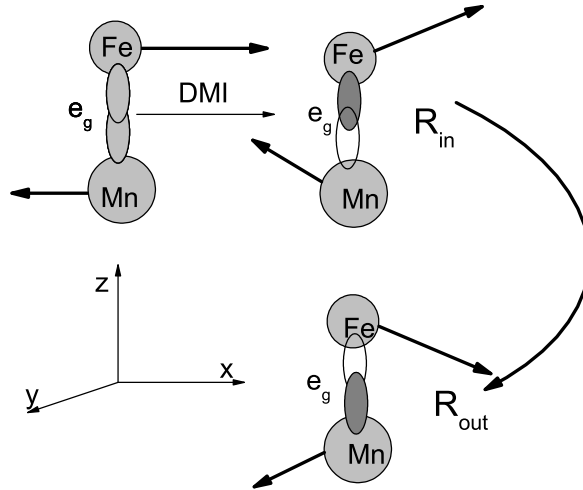


Fig. 5. Schematic diagram for rotation of magnetization and DMI between the neighboring Fe and Mn ions in  $\text{Bi}_2\text{FeMnO}_6$ . The arrow denote the magnetic moment.